Archiwum Instytutu Techniki Cieplnej Vol. **3** (2017) www.itc.polsl.pl/ArchiwumITC

Identification and modelling of the pulsatile blood flow in section of elastic large blood vessel

Marcin Nowak[1][2]
Instytut Techniki Cieplnej, Politechnika Śląska

e-mail: marcin9.nowak3@gmail.com

Key words: CFD, FSI, blood flow, aorta, vessel compliance

Abstract

Modelling of the blood flow process using computational fluid dynamics (CFD) and finite element method (FEM) can improve considerably understanding, diagnosis and prevention of cardiovascular diseases in non-invasively way. Moreover, studying of processes inside human body helps to develop products that interacts with organism. For example, automotive and sport industry find it very useful for designing their products, reducing the cost for R&D at the same time.

The aim of this study is to create a model of the blood flow in elastic blood vessel. Assumption of rigid blood vessel wall decreases the correctness of results, especially when the vessel undergoes quite large deformations. During cardiac cycle, the fluid flow induces forces from the time-varying blood pressure and wall shear stress. These forces causes strains of elastic vessels, which result in modification of the flow area. This was the motivation of using Fluid-Structure-Interaction (FSI) method.

In this research a real geometry model from 8-year old female patient with a moderate thoracic aortic coarctation (CoA) was analyzed. The geometry was obtained by gadolinium-enhanced Magnetic Resonance Angiography (MRA). Model includes ascending aorta, arch of aorta, descending aorta, brachiocephalic artery with right subclavian and right common carotid artery, left common carotid artery, left subclavian artery. Due to the lack of the detailed

[1] This chapter was prepared during master thesis project at the Institute of Thermal Technology, Department of Energy and Environmental Engineering of the Silesian University of Technology, under the supervision of Dr Ziemowit Ostrowski.

[2] This research is supported by National Science Centre, Poland, within project No 2014/13/B/ST8/04225 and No 2014/15/D/ST8/02620 (usage of GeoMagic Design X software). This help is gratefully acknowledged herewith.

data concerning arterial wall geometry, the wall thickness was calculated as 10% of the effective vessel radius.

The simulation was performed using 2-way iteratively implicit approach of FSI. This approach couples two numerical solvers: ANSYS Mechanical (Finite Element Method) and ANSYS Fluent (Finite Volume Method).

Pulsatile flow profile was implemented via User Defined Function (UDF) to mimic the cardiac cycle. This UDF consist of five polynomials created on twenty measuring points. The blood flow was modelled as laminar, single-phase, using non-Newtonian Carreau viscosity model.

1. Introduction

Many diseases related to cardiovascular system, such as atherosclerosis, high blood pressure, strokes causes deaths all over the world. In vivo studies, which can give information about actual state, often fails because of the difficulty, time required and expenses [7]. This is the reason why the development of cardiovascular CFD plays a big role in the treatment and diagnosis [7].

The cardiovascular system consists of heart and many blood vessels – arteries, small arteries, arterioles, capillaries and veins [9,10]. Reliable simulation of the whole system would be a very challenging task, which includes pulsatile flow, multiphase model, vessel elasticity and proper outlet boundary condition formulation (Windkessel effect [3,5]); it demands tremendous computing power. Thus, a model created within current research contains several limitations, like multiphase model omission (blood properties are averaged) and usage of just a fragment of cardiovascular system, described above.

The hemodynamic cardiac cycle comprises generation of changes of the blood pressure and blood volume in heart. It consists of several successive stages [9]:

- atrial systole
- isovolumetric contraction
- ventricular ejection
- isovolumetric relaxation
- ventricular filling

The whole cycle was possible to mimic using the blood flow information, acquired by cardiac-gated, 2D, respiratory compensated, phase-contrast (PC) cine sequence with through-plane velocity encoding [17]. The cardiac output was 86 beats per minute (i.e. cardiac cycle=0.7 s.). The inlet volumetric flow rate is shown in Fig. 1.

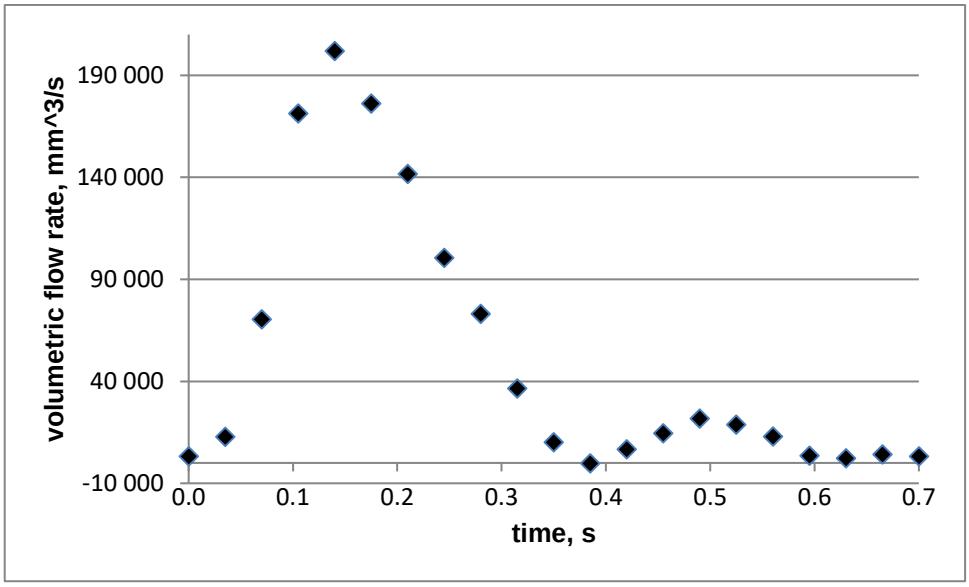

Figure 1. Ascending aortic flow

1.1 The scope of the research

The scope of the research comprise a model of the blood flow in truncated vascular system – ascending aorta, arch, descending aorta and upper branch vessels. The model includes vessel compliance and pulsatile inflow boundary condition. The blood was modelled as non-Newtonian. The geometry of vessels has to be created independently before the simulation. Assumptions of wall thickness as 10% of the medium local radius and composition of one vessel layer with averaged material properties were made.

1.2 Used software

The scanned data (.stl mesh file) were edited in Geomagic Design X (3D Systems Corporation) – including surface creation and wall addition.

For modelling numerical problems, commercial CFD software – ANSYS v. 17.2 was used. It includes the module for operating with geometry (DesignModeller, SpaceClaim), meshing (ANSYS Meshing) and solving (Fluent and Mechanical – APDL). System Coupling was the segment enabling communication between structural and fluid solver, including simulation setup, making appropriate data transfers, monitoring convergence between solvers and inside them and monitors tracking.

1.3 Fluid-structure interaction

Fluid-structure interaction can be used when the fluid flow interact with the solid body, exerting pressure and/or thermal load [2]. This pressure produces force, which causes deformations of solid, and by that – fluid domain. When deformations may be neglected on the fluid side, 1-

way approach can be used, where solution from one field is used as a boundary condition or external load for the second one.

2-way approach is used, when deformations are significant enough to change the flow field.

There are two methods of performing this approach. The first, fully coupled, solves fluid and solid equations in a single monolithic matrix, which is very difficult and not available using ANSYS software [2]. The second, which was used in this paper, is partitioned approach (iteratively implicit). It couples two numerical solvers: ANSYS Mechanical (Finite Element Method) and ANSYS Fluent (Finite Volume Method). After obtaining solution from Mechanical solver, the information about the displacements is transferred via previously created fluid-solid interface to the Fluent solver. This solver calculate forces and displacements (via dynamic mesh) and transfer them back to the Mechanical. This sequence is presented in Fig. 2 and is repeated within each time step until the results between two different fields are converged, i.e. the normalized change between data transfer values is below 0.01 [2,13]. The first coupling iteration of the first time step is slightly different – it begins with the Fluent initialization and transferring values to the Mechanical, and then the actions are exactly the same.

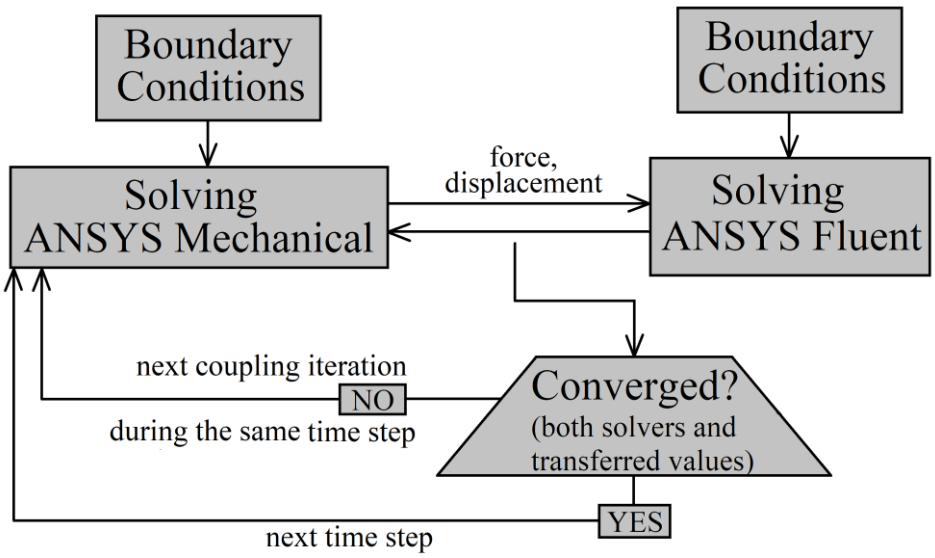

Figure 2. Flowchart of the 2-way iteratively implicit approach

2. Geometry model

2.1 Geometry data source

The geometry of 8-year old patient's aorta with congenital coarctation (approx. 65% area reduction) was used. During the MRA acquisition the subject was holding supine position and breath paused. The .stl file comprises 114,514 faces and 57,259 points [17].

2.2 CAD geometry creation

The method applied for geometry acquisition provide only fluid region, so the first task of geometry preparation was to create a variable-thickness solid domain, which was made using Geomagic Design X program. There are several different approaches for determining wall thickness, noted in [1,4,14]. Alishahi M. M. et al imposed constant thickness – 1 mm for abdominal and 0.5 mm for iliac region. Reymond P. et al were using thickness model that include patient age and outer diameter. In this paper, the solid geometry was created assuming wall thickness as 10% of the local effective radius [4]. For this purpose, the fluid domain was divided into nine regions with approximate equal lumen diameters presented in Fig. 3.

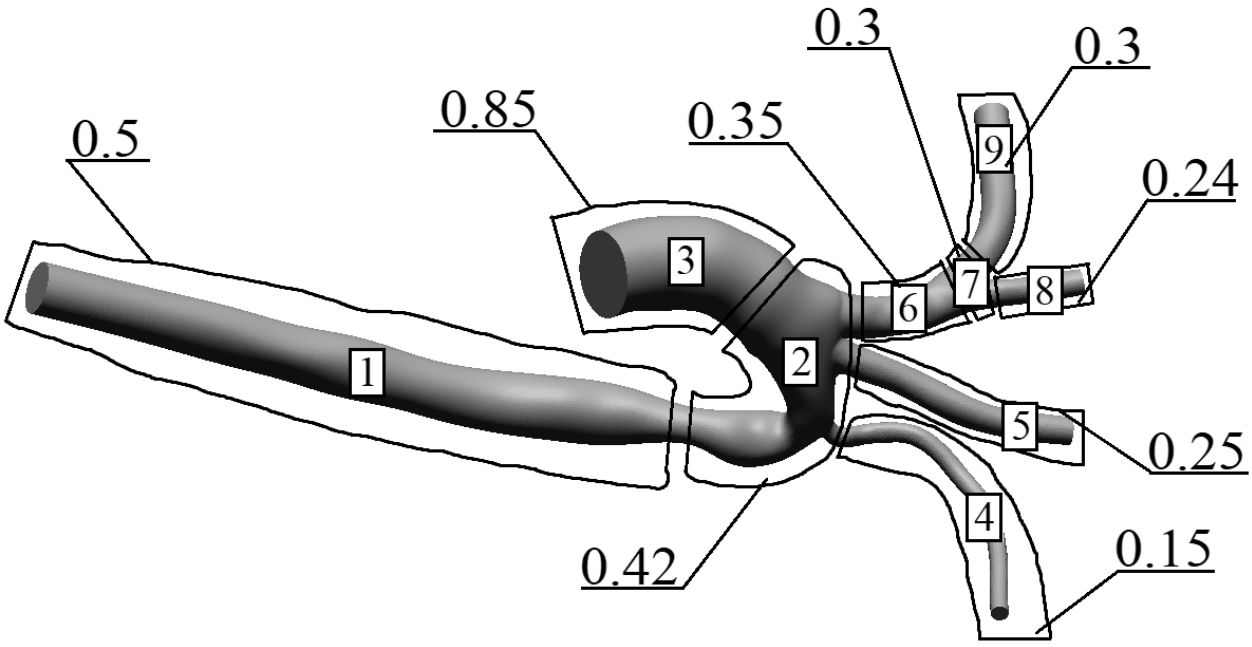

Figure 3. Solid wall thickness distribution in the numerical domain [mm]

The thickness of region 2nd and 7th was calculated as an arithmetic average of surrounding areas, i.e. number of 1, 3, 4, 5, 6 and 6, 8, 9, respectively. The minimum thickness defined was equal 0.15 mm, and maximum 0.85 mm.

Each region required creating of independent file. After importing .stl geometry and mesh optimizing (e.g. high quality conversion or sharp edges modifying), the inner wall surface was created via loft operation or autosurfacing. The last one was used only for high irregular regions, like aortic arch or bifurcation. Then, the thickness was added using thicken operation. However, it was impossible for autosurface regions, because some faces had the radius of curvature lower than thickness added. For these two regions, the outer wall surface had to be created using mesh-thicken and then autosurface operation on thickened mesh. Afterwards, inner and outer surfaces were connected and the solid body was achieved.

After obtaining nine solid domains, every solid body was exported via .igs file and then imported to the one new Geomagic file. The last stage was to connect regions into one. For this purpose, several connecting solid walls were created in way that ensure smooth transition between adjacent thicknesses. Exemplary connector merging region 1 and 2 is shown in Figure 4.

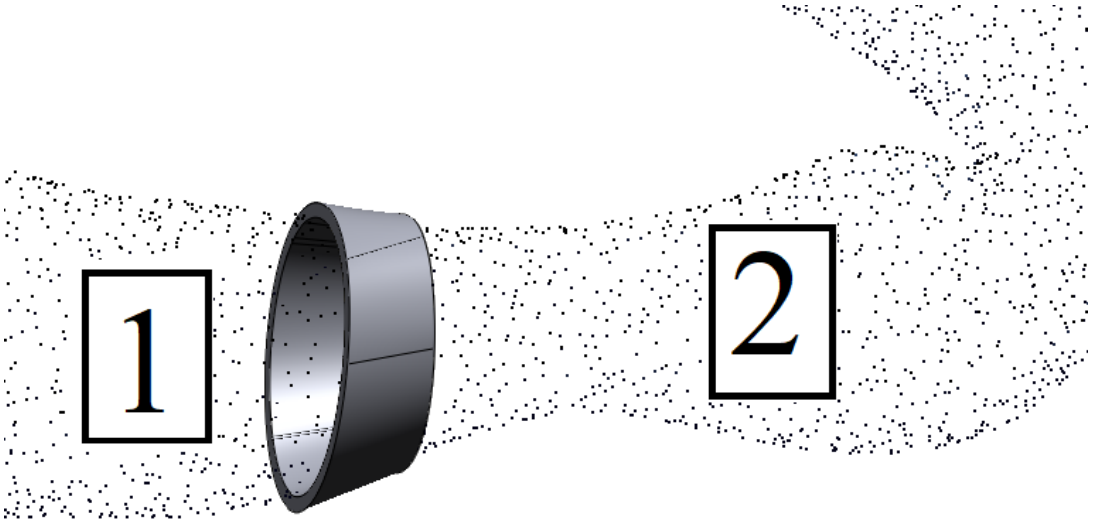

Figure 4. Connector merging two regions with different wall thicknesses

The last stage was repairing solid geometry prepared in Geomagic, using SpaceClaim. It included mainly elimination of inexact edges (gaps), small faces and faces merging. Without repairing, the numerical mesh contained many narrow faces, which imposed unjustified local mesh refinement. These places could have high smoothness (cell size change), which may cause some numerical errors [15].

2.3 Fluid geometry

The fluid geometry was created in DesignModeller via operation fill by cavity, using previously created solid domain.

The final solid and fluid domain are shown in Figure 5.

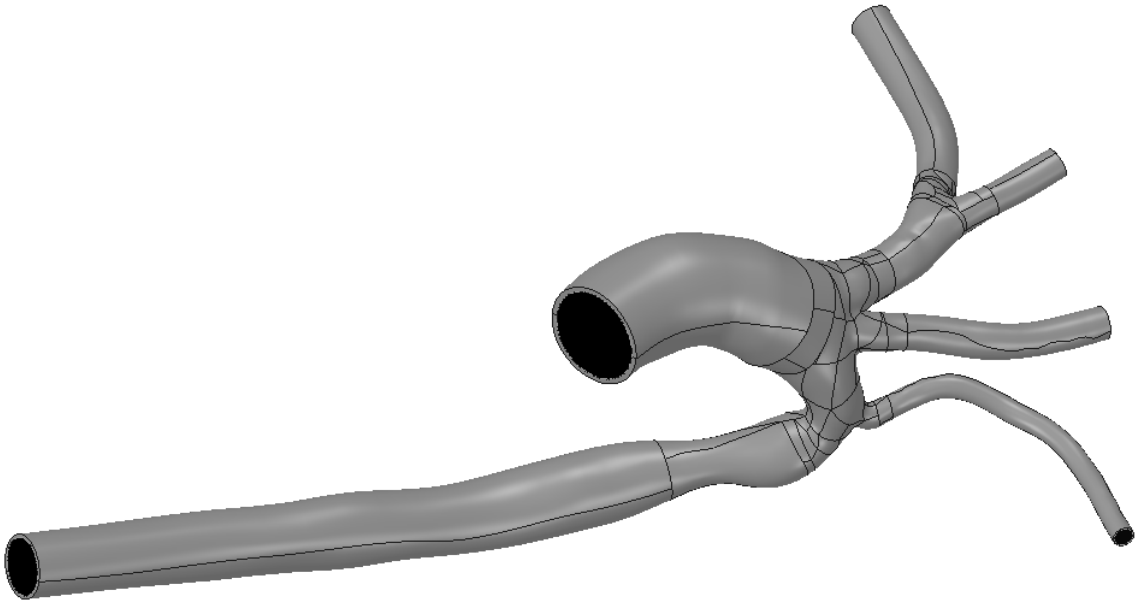

Figure 5. Solid domain (grey color) and obscured fluid domain (black color)

3. Numerical model and simulation setup

3.1 Fluid domain

In this work, governing equations applied in Fluent, which included mass and momentum conservation equations, were used.

The blood was modeled like single-phase, non-Newtonian liquid. It means that the shear stress is not linearly dependent with shear rate. The Carrou model [6] was implemented using eq. (1).

$$\eta = \eta_\infty + (\eta_0 - \eta_\infty) \cdot \left[1 + (\lambda\dot{\gamma})^2\right]^{\frac{n-1}{2}} \quad (1)$$

where:

η – non-Newtonian viscosity
$\eta_0 = 0.056\ Pa \cdot \mathrm{s}$ – zero-shear-rate viscosity
$\eta_\infty = 0.00345\ Pa \cdot \mathrm{s}$ – infinite-shear-rate viscosity
$\lambda = 3.313\ s$ – characteristic time
$n = 0.3568$ – power-law index

The blood density was assumed as $1051\ \frac{kg}{m^3}$ [11, 12].

For velocity-inlet boundary condition, UDF containing five polynomials was implemented. For one of 20 measuring points, where the flow rate was negative, it was assumed equal 0 kg/s. Inflow boundary condition has got the possibility of the negative velocity, but the intent was to avoid instability problems. The final inlet velocity profile, created from the measuring points, is shown in Fig. 6, where the area-weighted average monitor was recorded.

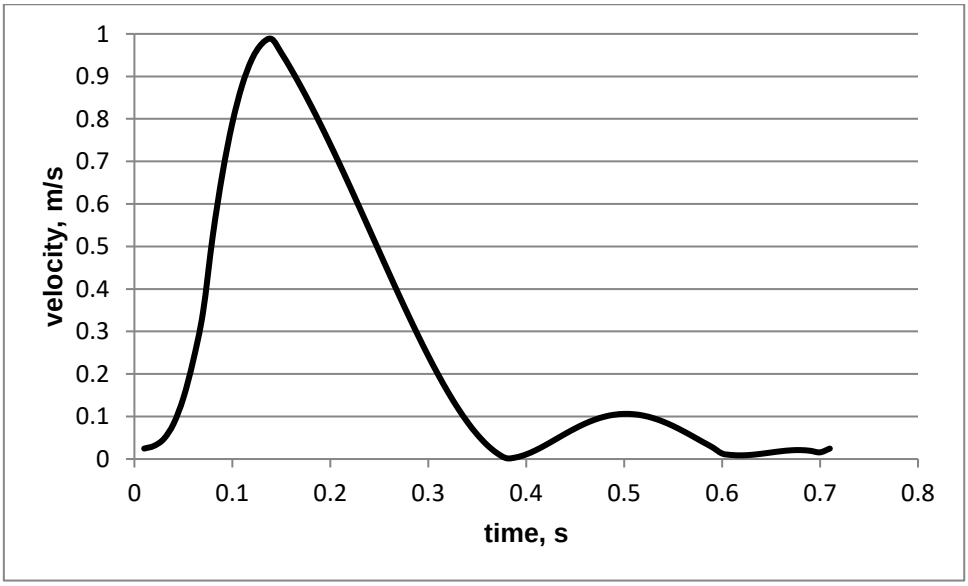

Figure 6. Velocity inlet, area-weighted average

For each of 5 outlets, the pressure-outlet boundary condition was assumed with constant pressure on the level of 0 Pa.

3.2 Solid domain

The blood vessels consist of three layers: intima, media, adventitia [3, 8]. In this paper one averaged layer was assumed with Young modulus E=1.7 MPa, Poisson ratio ν=0.45 and density 1100 $\frac{kg}{m^3}$ [13].

In ANSYS Mechanical, fixed support condition was used for every vessel ending cross-section.

3.3 Fluent and Mechanical tests

Before the coupled analysis, it is important to perform tests on individual solvers to detect and fix possible problems not related with FSI.

For the transient Fluent test, a tetrahedron numerical mesh with 4-element boundary layer and about 860k elements was used (after several Fluent mesh tests). A constant velocity 1 m/s was entered (close to maximum in the cardiac cycle). Calculations were successful and converged.

In Mechanical test, additional boundary condition of internal pressure was used, to mimic the pressure during blood flow.

These tests let to determine possible maximum pressure during cycle and maximum pressure in Mechanical which do not cause excessive element distortion. The influence of solid domain mesh on the maximum possible pressure was investigated and the optimal mesh was chosen. Moreover, it gave information about displacement distribution resulting from the level of internal pressure.

3.4 Preparing coupled analysis

3.4.1. Dynamic mesh

To receive displacement on the fluid side, the dynamic mesh has to be enabled and set. There are three different methods:

- Smoothing method, which moves interior nodes to absorb the motion of a moving or deforming boundary;
- Remeshing method, which creates locally a new mesh and makes it possible to simulate large relative motion and produce better quality mesh. It is possible only for tri, tet and extruded tri elements;
- Layering method, which adds and removes layers of cells adjacent to the deforming zone.

For determining the best method for this case, and save computing power at the same time, the new Fluent case with UFD was created. It includes only part of descending aorta, because of the necessity of assigning in UDF one coordinate system whose axis could contain the whole geometry. The UDF that was developed moves nodes of the exterior blood layer to mimic deformation without any lengthy, time-consuming calculations. Using the preview mesh motion method, the best dynamic mesh parameters were chosen.

Two methods were implemented: smoothing and remeshing. Firstly, Fluent tries to move nodes (smoothing). When the elements exceeds allowable value of the skewness parameter (set 0.7) the remeshing is invoked.

Other test shows that using structural, hex mesh cannot be used here, because deformations are too high to use only layering and smoothing – two methods applicable for hex meshes. Every attempt resulted here in the negative cell volume (NCV) problem.

3.4.2 Fluid and solid numerical meshes

After individual solvers setup and creating appropriate data transfers (force and displacement), the coupled analysis was tested with time step size equal 0.01 s. The selected Fluent mesh in coupled analysis turned out inadequate due to the problems with obtaining properly low continuity and coupling residuals. The most likely reason was too thick boundary layer on upper-branch vessels. This layer consists of the prism elements that could only be smoothed. For this reason, the mesh with variable thickness of the boundary layer, i.e. 8% of the local radius, was prepared.

The second possible reason of residuals problem was too coarse mesh on upper branches. Thus, the maximum cell size in this region was reduced using sphere of influence.

The unstructured mesh, showed in Fig. 7, consists of 1.25 million elements. It is easy to observe, that the element size is lower in the upper-branch vessels and the boundary layer has a very similar thickness comparing with the local lumen diameter.

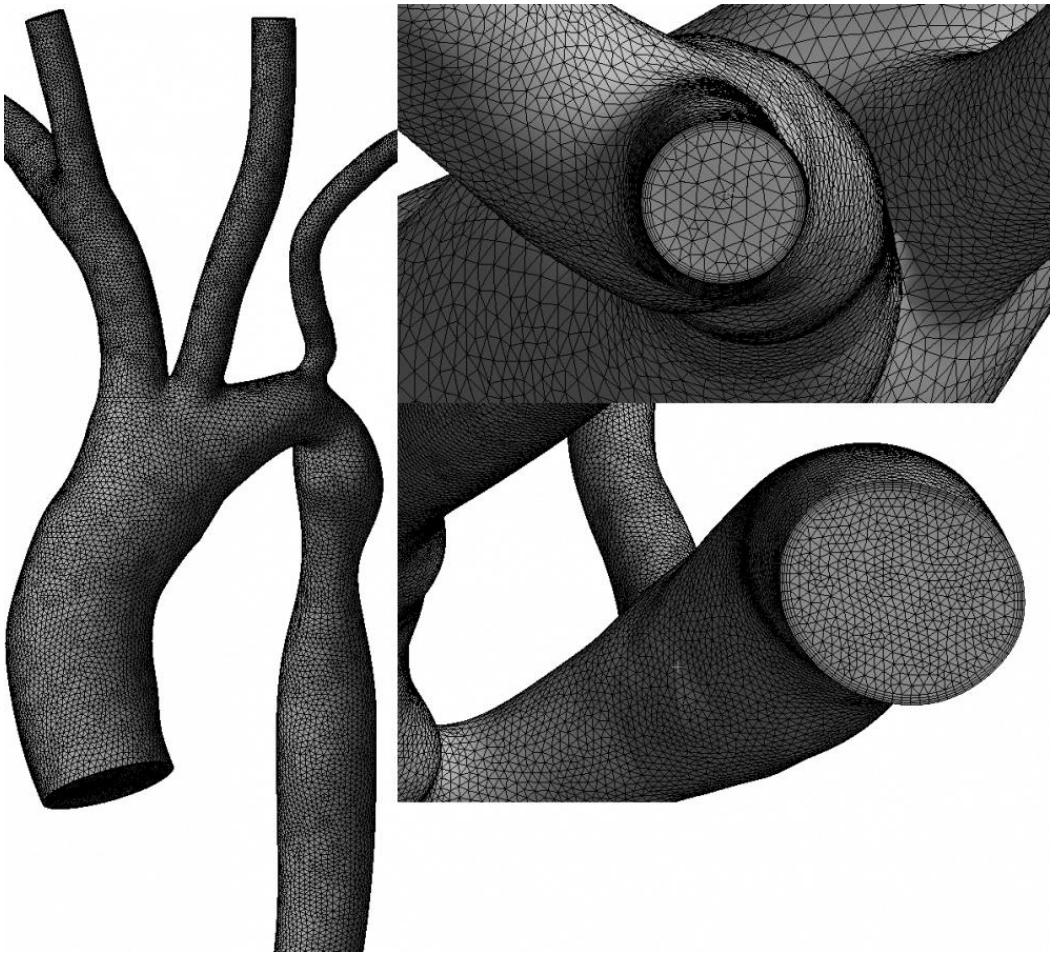

Figure 7. Mesh of the fluid domain

Before the simulation has been starting, the element quality and skewness of the fluid mesh had been verified. Fig. 8 and 9 shows the percent mesh volume with the specific value of indicator. It has been found, that the fluid mesh is appropriate.

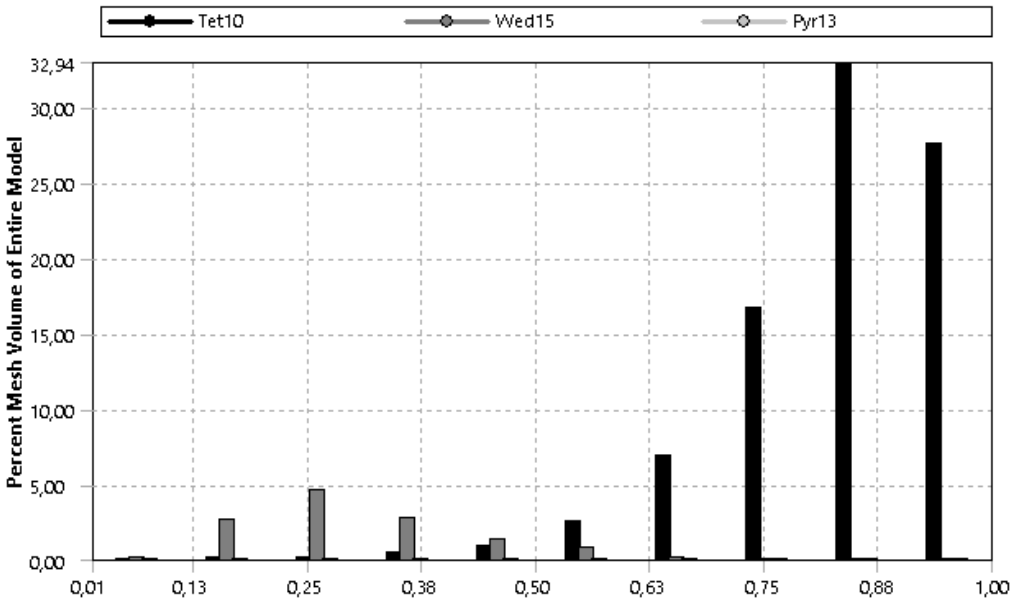

Figure 8. Element quality

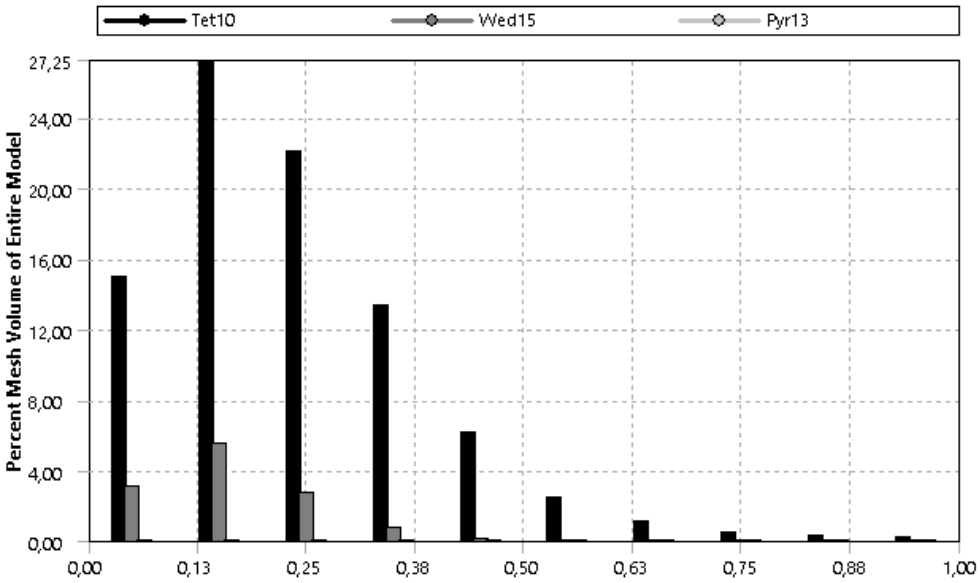

Figure 9. Element skewness

The solid body mesh should consist of large enough number of elements, because of the necessity of good matching between solid and fluid meshes. Coarse meshes with surface curvature can lead to force and displacement transfer problems [2]. Moreover, it has to coincide with the conclusions made during Mechanical test, i.e. the solid mesh cannot be too dense

because of the element distortion problems. Finally, the unstructured solid mesh consists of 90k elements and 180k nodes and is presented in Fig. 10.

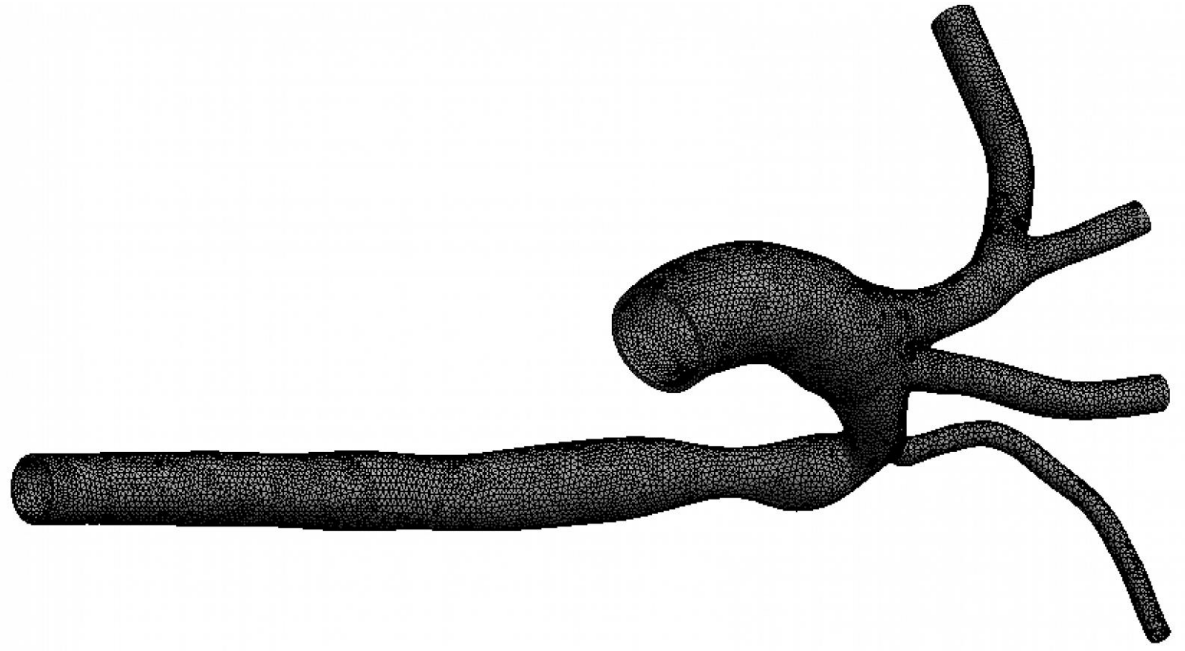

Figure 10. Mesh of the solid domain

3.4.3 Simulation process

During the simulation, many problems occurred, related to field or coupling convergence and excessive element distortion in Mechanical. It is caused by:

- highly flexible structure of solid body
- dense, incompressible liquid
- time-varying velocity

Since the first coupling iteration, after Fluent initializing, the forces are passed to Mechanical. Then, due to the fluid pressure, the solid domain extends and displacements are passed to Fluent. The volume increases, so the pressure in Fluent decreases and the forces are transferred again to the FEM Solver. In the second coupling iteration, the solid deforms in the opposite direction. Described process is repeated.

The simulation required proper selection of many controls to obtain good, converged results:

- proper initialization
- using solution stabilization (here: volume-based)
- choosing an appropriate time step size and number of Fluent iteration per step

- Under Relaxation Factors
- adequate fluid and solid meshes (type, number of elements, proper matching between meshes)
- dynamic mesh parameters

Three time step sizes were used during the calculations: 0.01 s, 0.0075 s, 0.005 s and their synchronization with the specific flow time is presented in Tab. 1.

Table 1. Time step sizes used in the simulation

Flow time	Time step size
0.01-0.14	0.01
0.14-0.27	0.005
0.27-0.2775	0.0075
0.2775-0.4325	0.005
0.4325-0.7025	0.0075

Three Fluent monitors were tracked: maximum and medium wall pressure and wall pressure integral (equivalent with the force). The solution convergence was investigated based on the residuals, mass balance and the constancy of already mentioned monitors in the last iterations. It was checked, that the values transferred between solvers (force and displacement) were also converged – the relative change (RMS parameter) in the last coupling iteration of the every timestep was below 1%.

4. Results

The results that follows represents the static pressure distribution on the wall of the fluid domain.

Figure 11. shows the pressure during two characteristic points in cardiac cycle – systole (0.14 s) and diastole (0.62 s). In both cases the highest pressure occurred in the inlet area and was on the level of 4300 Pa (systole) and 200 Pa (diastole). The difference between the maximum and minimum pressure was 4560 Pa for systole and 202 Pa for diastole.

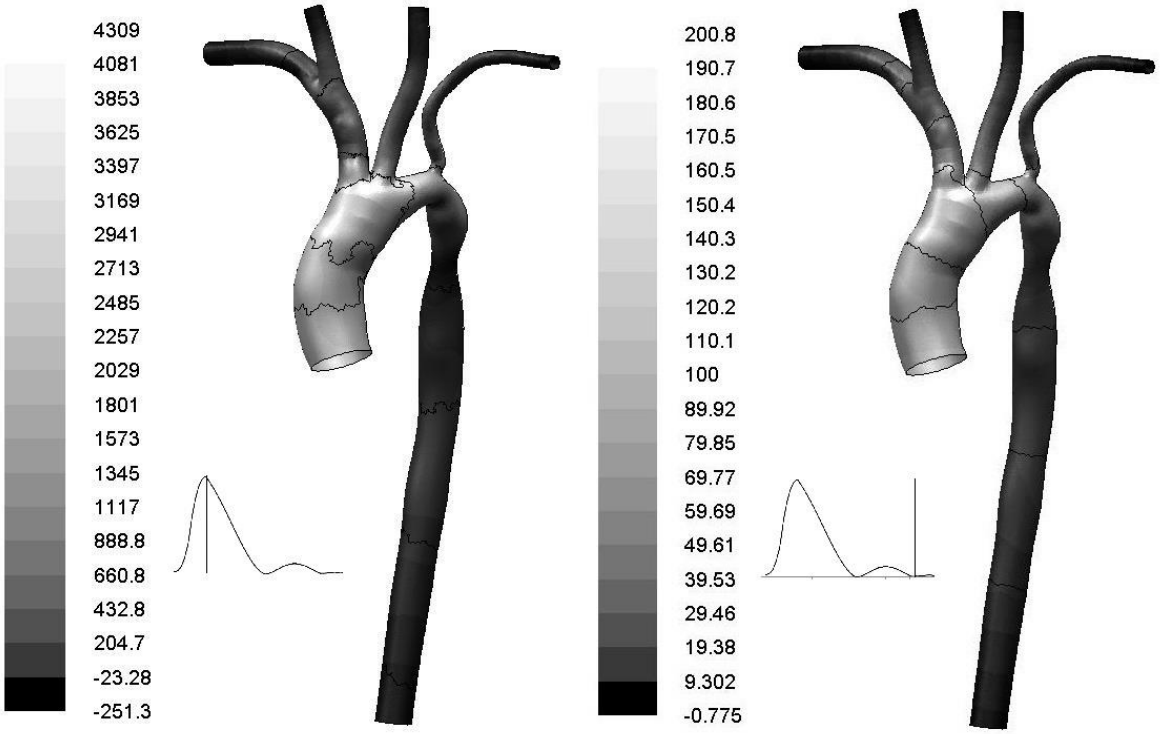

Figure 11. Wall pressure comparison between the systole (0.14 s) and diastole (0.62 s)

Figure 12. describe the moments when the maximum and minimum pressure appeared in the cycle. The maximum value, about 4600 Pa, occur the moment before the velocity peak. The minimum value, -1800 Pa, was when the velocity was decreasing (0.185 s).

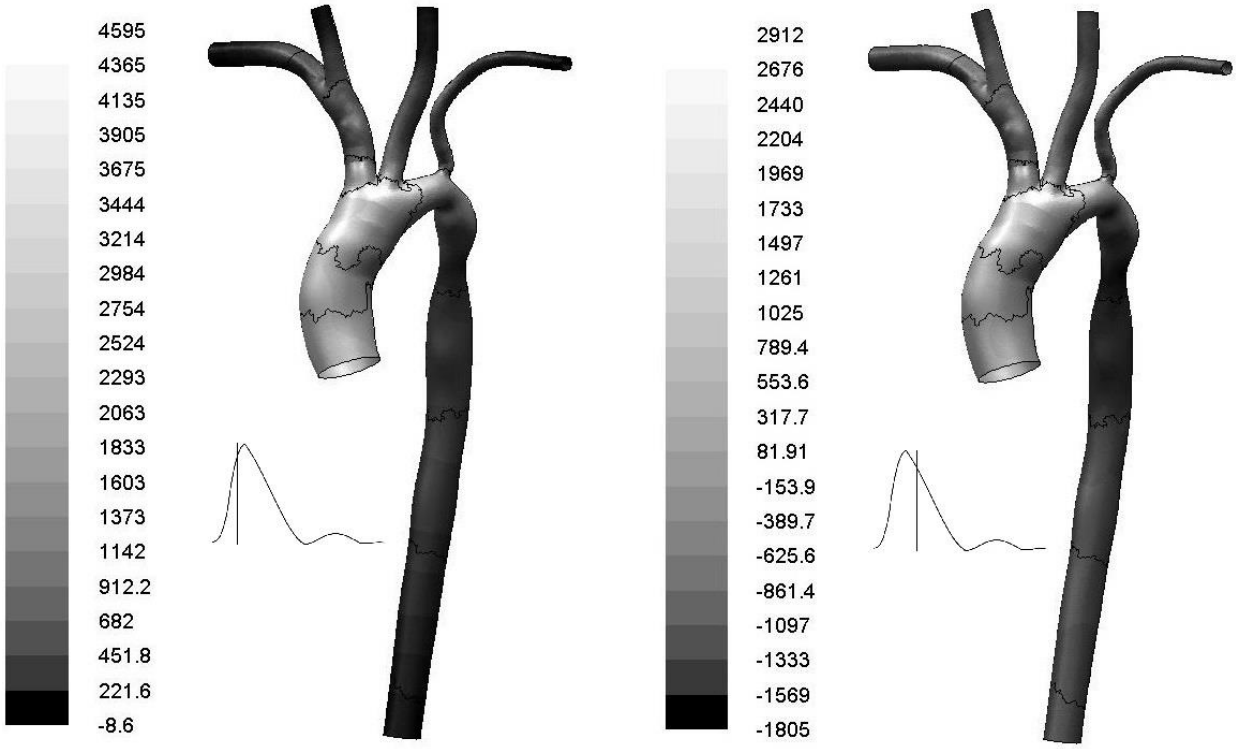

Figure 12. Wall pressure comparison between the maximum (0.11 s) and minimum (0.185 s) domain pressure moment.

The medium wall pressure was in the range of -300 Pa and 2150 Pa and is presented in Fig. 13. The function course is related with the inlet boundary condition (pulsatile blood flow). However, the maximum area-weighted average wall pressure was not in the moment of maximum inlet velocity, which was caused by the vessel deformations. The negative values occurred when the vessel was contracting, which can be observed and compared with the videos in the Appendix.

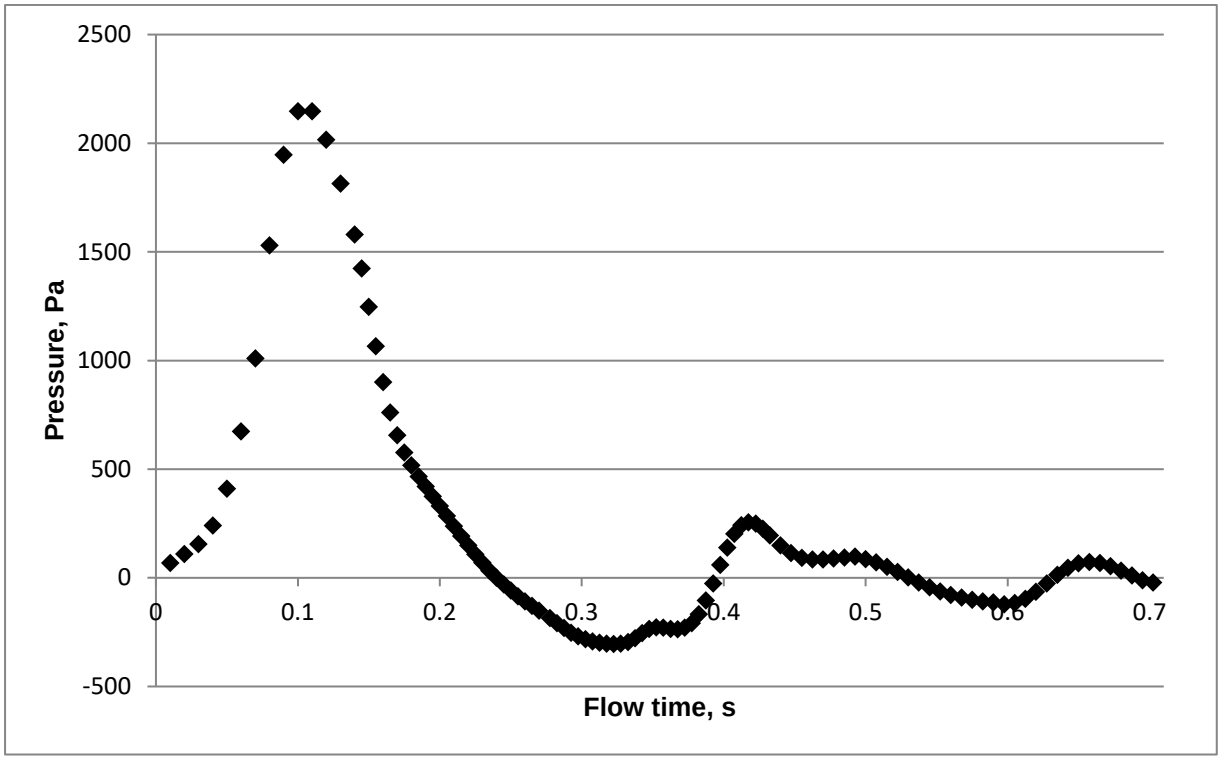

Figure 13. Area-weighted average of the wall pressure

Figure 14. shows the outlet velocities distribution during cardiac cycle. The maximum velocity of 2.25 m/s was in the moment of the systole in the right common carotid artery.

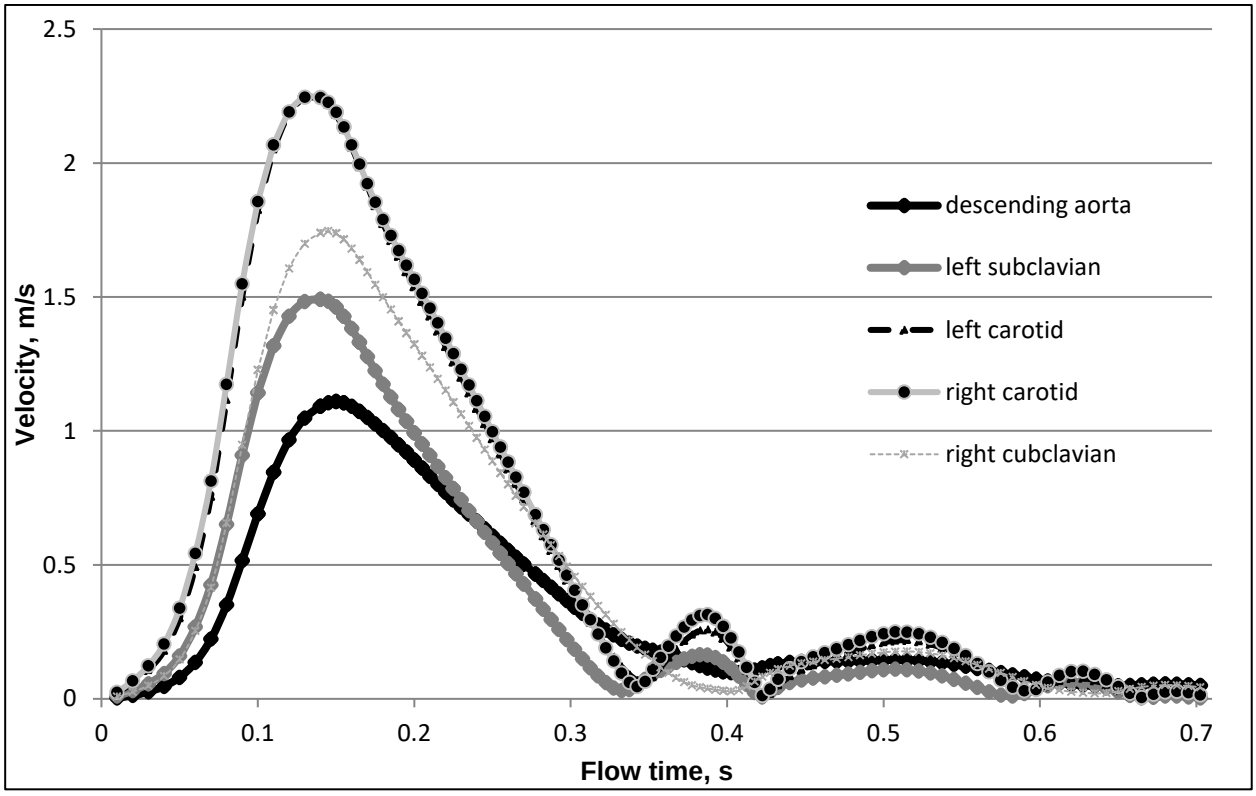

Figure 14. Area-weighted average of the outlet velocities

Figure 15. represents the velocity vectors on the sections of ascending and descending aorta during the systole and diastole. The ascending section seems to be almost laminar during the whole cycle. In turn, the descending one shows some vortices, starting from the velocity peak, which can be observed in attached video. The maximum velocity value was below 3 m/s.

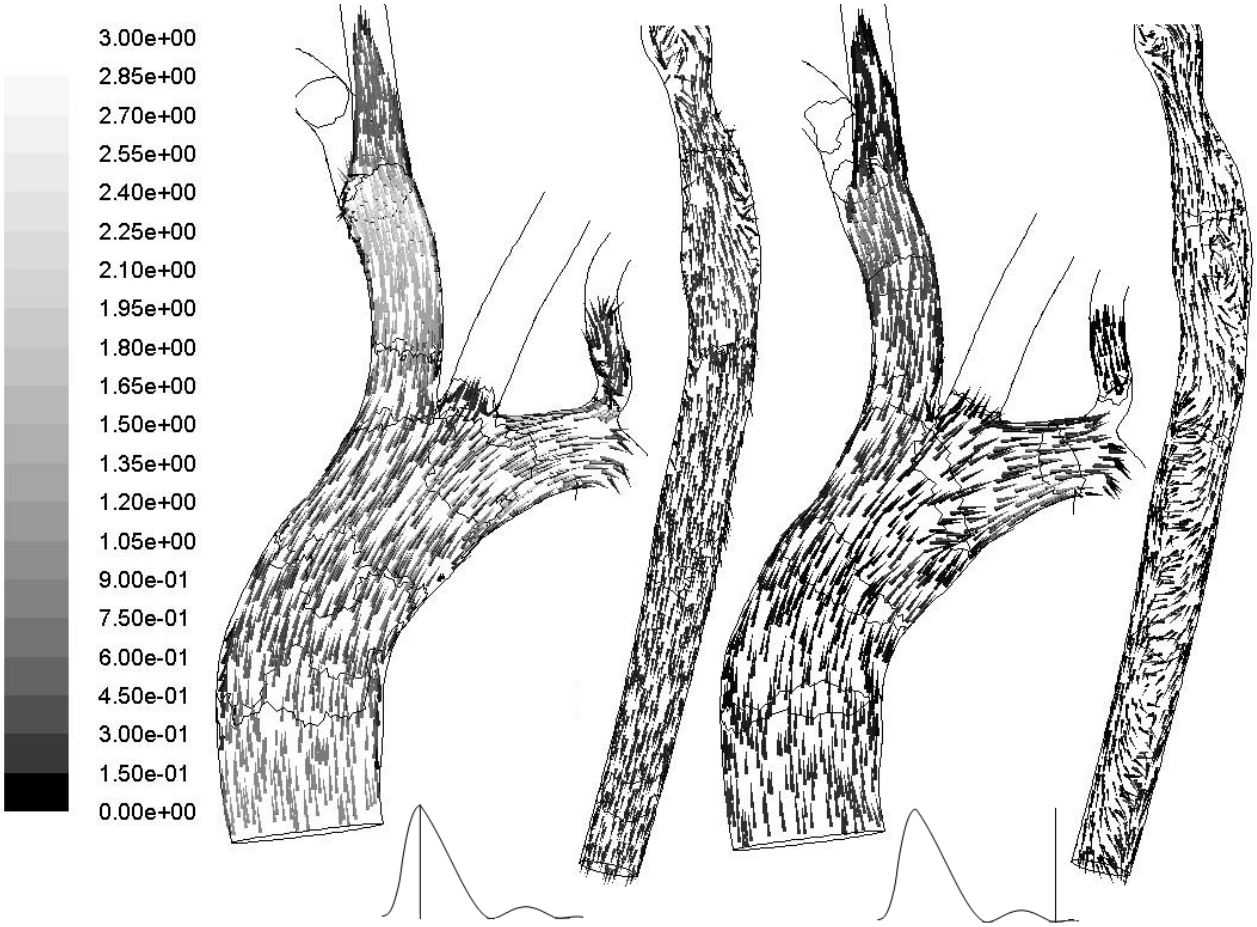

Figure 15. Velocity vectors during the systole and diastole

The wall shear stress (WSS), which is connected with the atherosclerosis formation, is a difficult to measure parameter. For this reason, the numerical simulations can help to assess the WSS distribution, using the patient-specific data [7].

The maximum value of the WSS achieved 160 Pa during 0.18 s and was located on the aortic bifurcation (Figure 16.). It was checked, that this region is related with the local maximum wall pressure during the whole cycle.

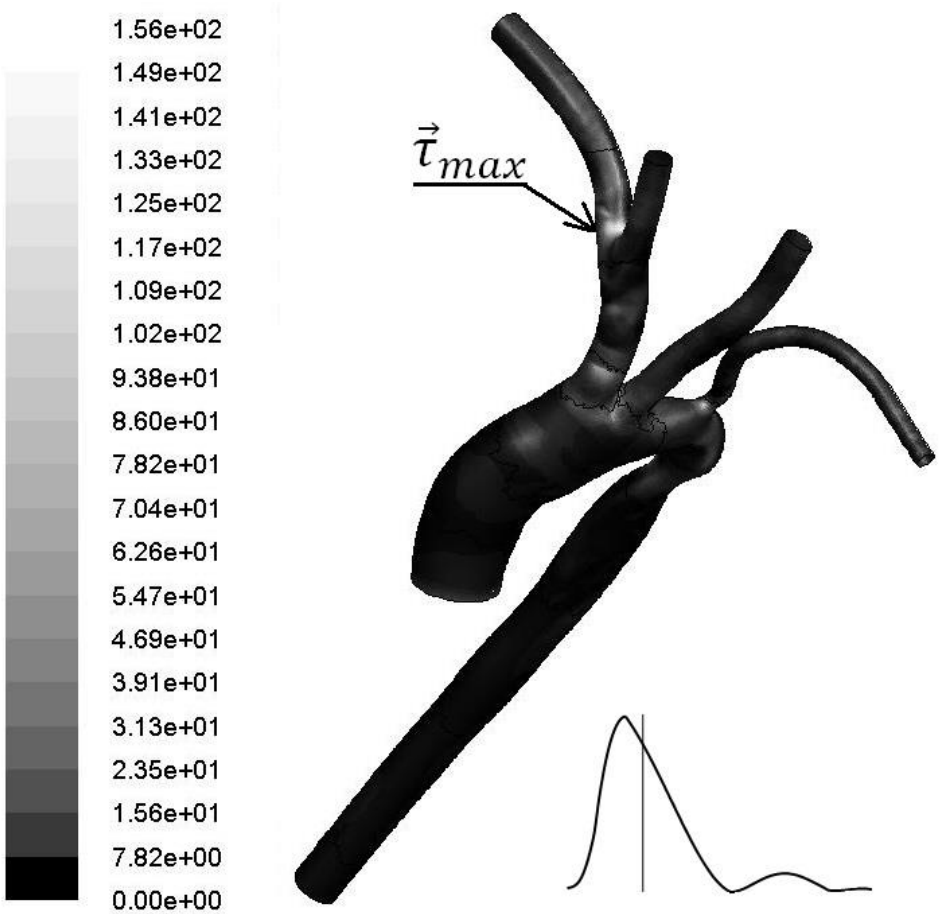

Figure 16. WSS distribution

Figure 17. represents the cross-sections of the descending aorta in the place of the coarctation. It contains nine, equally-distributed time moments and gives information about:

- dynamic mesh operation, which include smoothing of the boundary layer and both smoothing and remeshing of the rest area
- deformation of the vessel lumen
- aortic displacement that is an effect of the vessel flexible bending

The maximum deformation in presented cross-section can be observed in the moment of 0,2650 s.

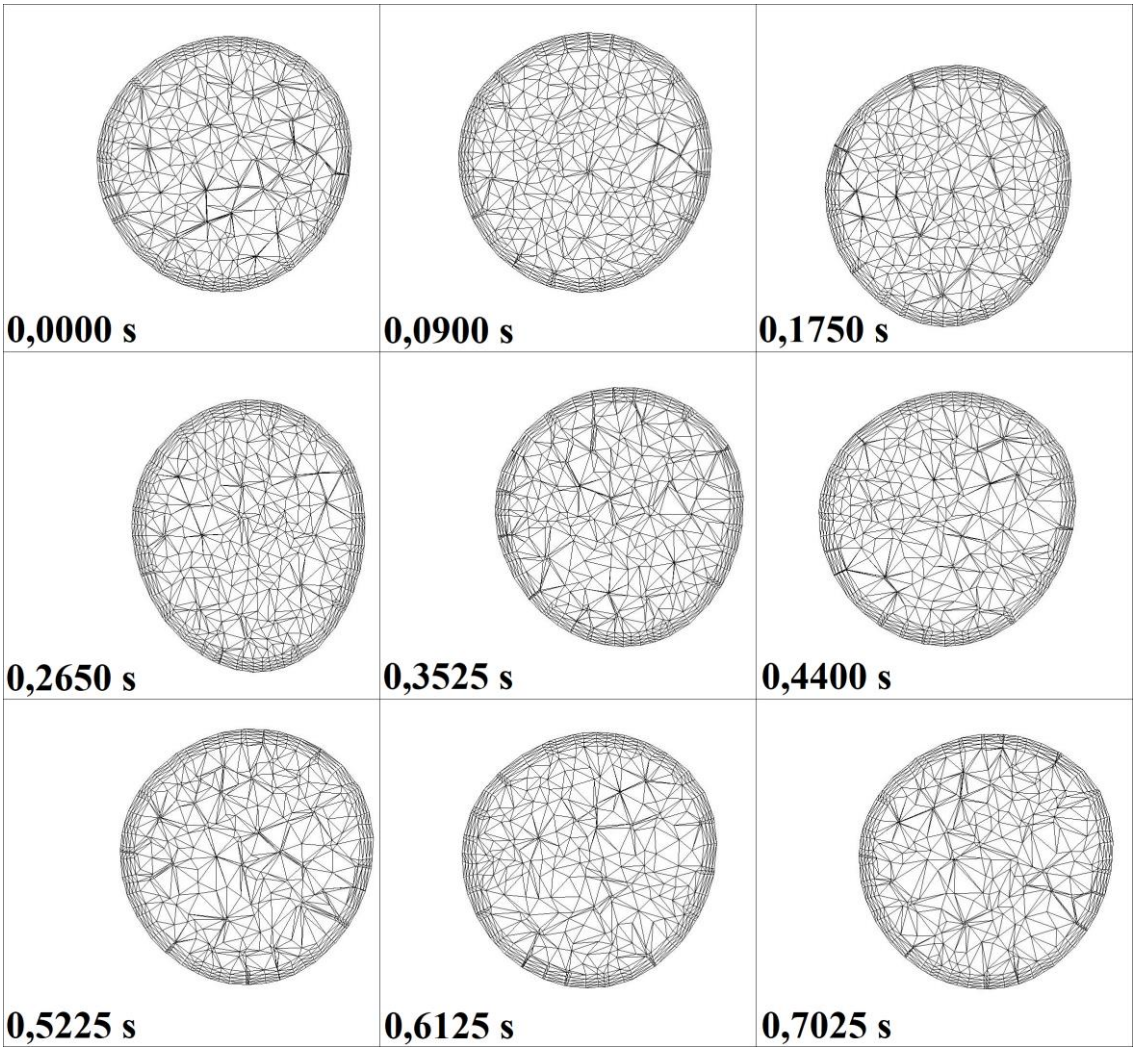

Figure 17. Aortic cross-section during several cycle moments

Fig. 18 shows ANSYS Mechanical results – the maximum of total vessel deformation during the cycle. The maximum value achieved 2.35 cm and was located in descending aorta, below the coarctation. This value is high comparing with the local vessel radius of 0,5 cm and is related to flexible vessel bending and cross-section areas changes.

Fig. 19 relates to the moment of maximum deformation (0.255 s) and shows its distribution on the solid domain. The major deformations are observed in the region of the descending aorta in the section behind coarctation. For detailed information please check the animations noted in the Appendix.

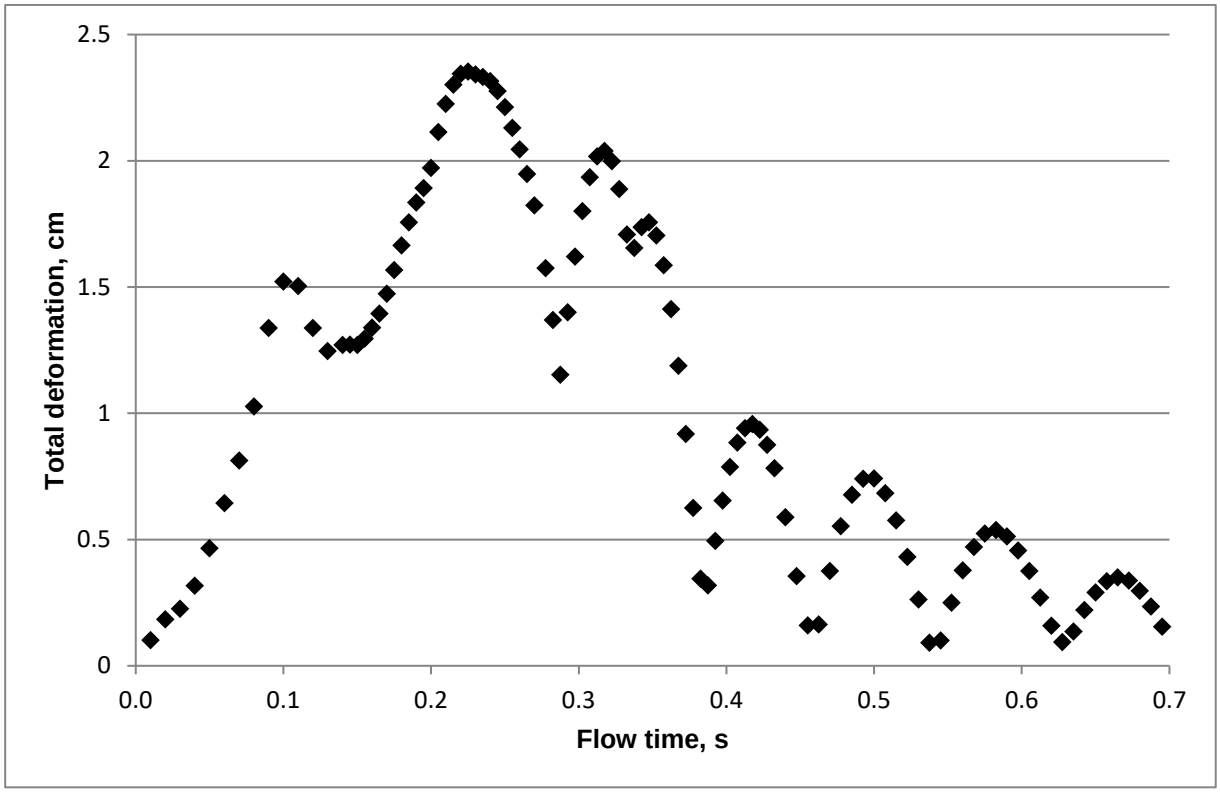

Figure 18. Maximum of total vessel deformation

5. Conclusions

The scope of this work was to conduct analysis of the blood flow in the human aorta section and its main branches, considering the vessel deformations, with using of the numerical simulation. This approach can improve the accuracy of the results comparing the rigid wall approach, especially when the vessel undergoes relatively high displacements. The simulations yield the maximum displacement reaching 2.35 cm, which confirms that taking into account the vessel compliance was reasonable.

The real geometry of 8-year old female patient was used.

The blood was modelled as a single-phase, non-Newtonian fluid with averaged material properties. The blood vessels were assumed as single layer with variable thickness.

The pulsatile blood flow was implemented using User Defined Function (UDF). The outlet boundary condition was simplified as 0 Pa pressure outlet. The most correct hemodynamic modelling should be connected with the electrical analogy [3,5].

The results showed in paper present the pressure, velocity and wall shear stress distribution. The operation of the dynamic mesh smoothing and remeshing was depictured. For mechanical results, the displacement distribution was discussed.

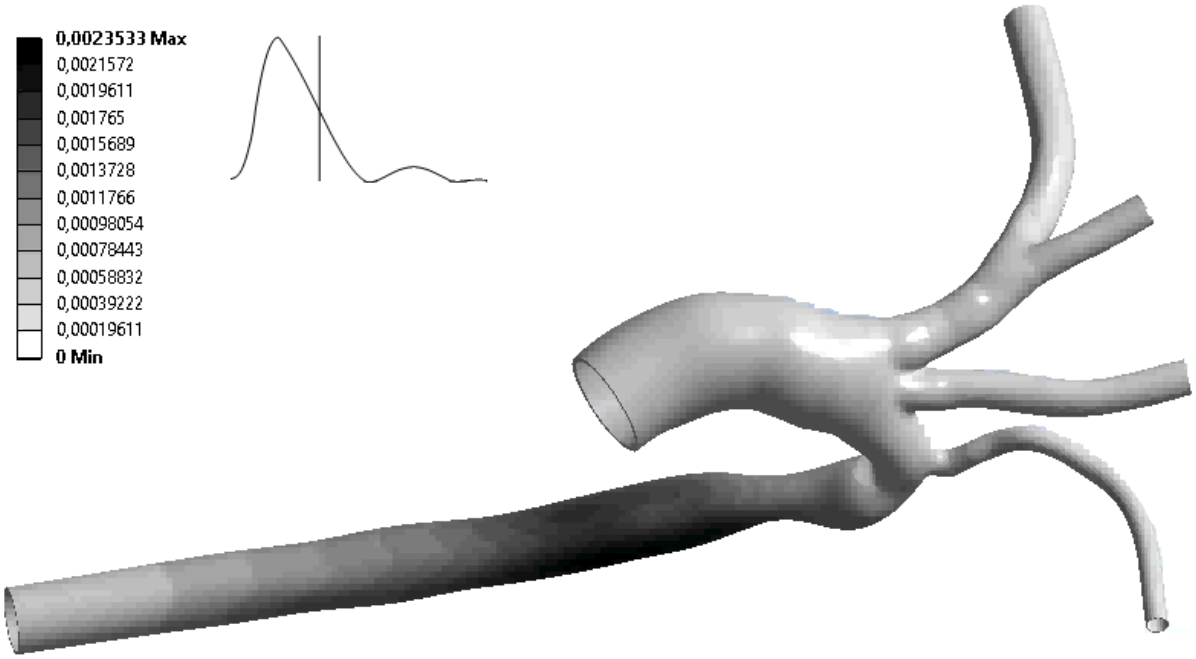

Figure 19. Distribution of the blood vessel deformations [m]

Acknowledgements

This research is supported by National Science Centre, Poland, within project No 2014/13/B/ST8/04225 and No 2014/15/D/ST8/02620. This help is gratefully acknowledged herewith.

I would like to express my sincere gratefulness to Bartłomiej Melka for his invaluable contribution and the long time spent together on this project.

I would also like to thank Dr Wojciech Adamczyk for the access to the Geomagic Design X software.

References

[1] Alishahi M. M. et al, Numerical simulation of blood flow in a flexible stenosed abdominal real aorta, Scientia Iranica B (2011) 18 (6), 1297–1305
[2] ANSYS Academic Research, Release 17.0; Help System, UDF Manual, System Coupling User's Guide, ANSYS, Inc.
[3] Bandoła D., Identification and modeling the pulsatile blood flow in the cardiovascular system using a zero-dimensional model in an electrical analogy, Archiwum Instytutu Techniki Cieplnej Vol. 1 nr 1(2016)
[4] Bazilevs Y., Takizawa K., Tezduyar T., Computational fluid-structure interaction . Methods and applications, Wiley series in computational mechanics, John Wiley & Sons, 2013
[5] Catanho M., Sinha M. Vijayan V., Model of Aortic Blood Flow Using the Windkessel Effect, 2012 [online] [access 27.06.2017]

http://isn.ucsd.edu/classes/beng221/problems/2012/BENG221_Project%20%20Catanho%20Sinha%20Vijayan.pdf
[6] Cho Young, Effects of the non-Newtonian viscosity of blood flows in a diseased arterial vessel. Part I: steady flows, Biorheology, February 1991
[7] Crosetto P. et al., Fluid-structure interaction simulation of aortic blood flow, Computers & Fluids 43 (2011) 46-57
[8] Geomagic Design X 2014 User Guide
[9] Górski J., Fizjologiczne podstawy wysiłku fizycznego, Wydawnictwo lekarskie PZWL, 2006
[10] Kahveci K., Becker B., A numerical model of pulsatile blood flow in compliant arteries of a truncated vascular system, International Communications in Heat and Mass Transfer 67 (2015) 51-58
[11] Kenner T., The measurement of blood density and its meaning, Basic Research in Cardiology (1989) 84:111-124
[12] Liu B., Tang D., Influence of non-Newtonian Properties of Blood on the Wall Shear-Stress in Human Atherosclerotic Right Coronary Arteries, Mol Cell Biomech (2011) 8(1):73-90, doi: 10.3970/mcb, 2011
[13] Neidlin M. et al., Investigation of hemodynamics during cardiopulmonary bypass: A multiscale Multiphysics fluid-structure-interaction study, Medical Engineering and Physics (2016) 38(4):380–390
[14] Reymond P. et al, Physiological simulation of blood flow in the aorta: Comparison of hemodynamic indices as predicted by 3-D FSI, 3-D rigid wall and 1-D models, Medical Engineering & Physics 35 (2013) 784– 791
[15] Versteeg H. K., Malalasekera W., An introduction to computational fluid dynamics, Pearson education, 2007
[16] BioVox.eu, Virtual Physiological Human [online] [access 1.06.2017] http://biovox.eu/insights/detail/your-body-modeled-in-a-computer
[17] CFD Challenge problem: http://www.vascularmodel.org/miccai2012 (accessed June 10th 2017)

Appendix A - Supplementary data

Supplementary media files are available to ilustrate choosen simulation results:

https://youtu.be/9bOZdJIiGVM

File 1: True scale deformations in a section of descending aorta. Location of described region is presented in the picture. The right corner shows the cross-section of the fluid domain, where can be observed: dynamic mesh operation (smoothing, re-meshing), vessel lumen deformation and aortic displacement. The lower left corner shows total deformation of the blood vessel.

https://youtu.be/z3XE3uGHoW8

Total deformation of the blood vessel magnified 8.8 times. The legend marks are unscaled.

https://youtu.be/FehKISgbns4

True scale deformation of the blood vessel.

https://youtu.be/eLLe_lTERJg

Velocity vectors in the cross-section of the ascending aorta.

https://youtu.be/cFBLW69ETys

Wall pressure. Dynamic mesh operation on the entire blood domain is also represented.

Identyfikacja i modelowanie pulsacyjnego przepływu krwi w odcinku dużego, elastycznego naczynia krwionośnego

Marcin Nowak
Instytut Techniki Cieplnej, Politechnika Śląska

Słowa kluczowe: CFD, FSI, przepływ krwi, aorta, odkształcalność naczyń

Streszczenie

Modelowanie procesu przepływu krwi oparte na numerycznej mechanice płynów oraz metodzie elementów skończonych może znacznie poprawić zrozumienie, diagnozę i profilaktykę chorób układu krążenia w sposób nieinwazyjny. Co więcej, analiza procesów zachodzących wewnątrz ludzkiego ciała pomaga w rozwoju produktów oddziałujących w pewien sposób na organizm. Przykładowo, w przemyśle samochodowym oraz sportowym jest ona niezwykle użyteczna na etapie projektowania produktu, jednocześnie zmniejszając nakład finansowy na badania i rozwój.

Celem niniejszego badania było utworzenie modelu przepływu krwi w elastycznym naczyniu krwionośnym. Założenie nieodkształcalności ścian obniża poprawność wyników, szczególnie, gdy naczynie poddawane jest stosunkowo dużym odkształceniom. Podczas cyklu pracy serca, przepływ płynu wywiera siły wynikające ze zmiennego w czasie ciśnienia krwi i naprężeń ścinających. Siły te powodują odkształcenia elastycznych naczyń, co skutkuje modyfikacją powierzchni przepływu. Proces ten był argumentem do użycia metody Fluid-Structure Interaction.

W badaniu wykorzystano rzeczywistą geometrię od ośmioletniej pacjentki z koarktacją części piersiowej aorty. Geometrię uzyskano na drodze wzmocnionej angiografii (MRA). Model zawiera aortę wstępującą, zstępującą, łuk aorty oraz górne odgałęzienia. Z powodu braku szczegółowych danych dotyczących geometrii ścian naczyń, ich grubość została założona jako 10% lokalnego promienia.

Symulacja została przeprowadzona przy użyciu obustronnego sprzężenia. Podejście to jest związane z dwiema aplikacjami: ANSYS Mechanical (Metoda Elementów Skończonych) oraz ANSYS Fluent (Metoda Objętości Skończonych).

Pulsacyjny profil przepływu krwi został zaimplementowany przy użyciu procedur definiowanych przez użytkownika (UDF – User Defined Function). Jest on złożony z pięciu wielomianów, utworzonych na bazie dwudziestu punktów pomiarowych. Przepływ krwi został zamodelowany jako jednofazowy, a płyn jako nienewtonowski (model Carreau).